DEPARTMENT OF ELECTRICAL AND COMPUTER ENGINEERING
COLLEGE OF ENGINEERING AND TECHNOLOGY
OLD DOMINION UNIVERSITY
NORFOLK, VIRGINIA 23529

STUDY OF DIAMOND FILM GROWTH AND PROPERTIES

By

Sacharial Albin, Principal Investigator

Final Report
For the period ended July 5, 1989

Prepared for
National Aeronautics and Space Administration
Langley Research Center
Hampton, Virginia 23665

Under
NASA Research Grant NAG-1-791
Mr. Robert V. Hess, Branch Head
FED-Laser Technology and Applications Branch

December 1990

Old Dominion University Research Foundation is a not-for-profit corporation closely affiliated with Old Dominion University and serves as the University's fiscal and administrative agent for sponsored programs.

Any questions or comments concerning the material contained in this report should be addressed to:

Executive Director
Old Dominion University Research Foundation
P. O. Box 6369
Norfolk, Virginia 23508-0369

Telephone: (804) 683-4293
Fax Number: (804) 683-5290

DEPARTMENT OF ELECTRICAL AND COMPUTER
ENGINEERING
COLLEGE OF ENGINEERING AND TECHNOLOGY
OLD DOMINION UNIVERSITY
NORFOLK, VIRGINIA 23529

STUDY OF DIAMOND FILM GROWTH AND PROPERTIES

By

Sacharial Albin, Principal Investigator

Final Report
For the period ended July 5, 1989

Prepared for
National Aeronautics and Space Administration
Langley Research Center
Hampton, Virginia 23665

Under
NASA Research Grant NAG-1-791
Mr. Robert V. Hess, Branch Head
FED-Laser Technology and Applications Branch

Submitted by the
Old Dominion University Research Foundation
P.O. Box 6369
Norfolk, Virginia 23508-0369

December 1990

Study of Diamond Film Growth and Properties

By

Dr. Sacharia Albin

SUMMARY

Diamond has many unique properties which are technologically important. Included in these properties are its wide bandgap, high refractive index, high thermal conductivity, hardness and resistivity. In thin film form, diamond will be useful in several applications of laser optics. The objective of the research program was to study diamond film growth and its properties in order to enhance the laser damage threshold of substrate materials.

1. Laser Induced Thermal Stress Parameter, R_T

Calculations were performed to evaluate laser induced thermal stress parameter, R_T of diamond. R_T can be used as a figure of merit for evaluating laser materials; higher the value of R_T, higher the laser induced damage threshold (LIDT) of a material. It is found that diamond has several orders of magnitude higher value for R_T compared to other materials. The presence of isolated impurities in diamond film does not reduce its LIDT significantly.

2. Diamond Film Growth

diamond films were grown using a microwave plasma enhanced chemical vapor deposition (MPECVD) system at various conditions of gas composition, pressure, temperature and substrate materials. A 0.5% CH_4 in H_2 at 20 torr was ideal to grow high quality diamond films on substrates maintained at 900 ^oC. The density of nucleation was an important factor controlling the growth rate and it was enhanced by abrading the surface of the substrates.

3. Diamond Film Characterization

The diamond films were polycrystalline which were characterized by scanning electron microscopy (SEM) and Raman scattering spectroscopy. The absorption of free-standing

films were also measured. The top surface of the growing film is always rough due to the facets of polycrystalline film while the back surface of the film replicates the substrate surface. The Raman spectra showed the presence of sp^3 (diamond) and sp^2 (graphite) bonded carbon in the films. The graphitic content increases the optical absorption of the film.

An analytical model based on two dimensional periodic heat flow was developed to calculate the effective in-plane (face parallel) diffusivity of a two layer system. The effective diffusivity of diamond/silicon samples was measured using a laser pulse technique which does not require special sample preparation. The model was applied to deduce the diffusivity of polycrystalline diamond films using the spatial dependence of phase and amplitude. Excellent agreement has been obtained for the thermal diffusivity values measured using the two methods. The thermal conductivity of the films were measured to be 13.5 W/cmK, which is better than that of a type Ia natural diamond.

4. LIDT Measurement

Laser induced damage experiments were performed on bare Si substrates, diamond film coated Si, and diamond film windows and a differential reflectometer system was developed to obtain a quantitative measure of LIDT. A high power pulsed Nd:YAG laser system at 1064 and 532 nm was used to induce damage on the samples. Significant improvements in the LIDT were obtained for diamond film coated Si compared to the bare Si substrates. In the case of diamond film windows, the value of LIDT was found to be around 620 MW/cm^2. The measured values of LIDT was considerably lower than the theoretical value. Stress due to the lattice mismatch between the diamond film and the substrate, graphitic, content and surface roughness are contributing factors for the reduction of LIDT.

TABLE OF CONTENTS

		PAGE
SUMMARY		i
LIST OF FIGURES		iv
LIST OF TABLES		v
1. INTRODUCTION		1
2. LASER INDUCED DAMAGE		3
2.1	Dielectric Breakdown	3
2.2	Damage due to Impurities	3
3. DIAMOND FILM GROWTH AND CHARACTERIZATION		6
3.1	Microwave PECVD System	6
3.2	Substrate Preparation	7
3.3	Diamond Film Growth	7
3.4	Diamond Film Growth using 0.5% Methane	8
3.5	Diamond Film Growth using 1% Methane	10
3.6	Diamond Film Characterization	12
3.7	Raman Spectroscopy	12
3.8	Absorbance Spectrum	14
3.9	Thermal Diffusivity of Diamond Films	15
3.10	Analysis	16
3.11	Thermal Diffusivity Measurement	19
4. LASER INDUCED DAMAGE THRESHOLD MEASUREMENT		24
5. FURTHER RESEARCH		29
5.1	High Density Nucleation	29
5.2	Low Temperature Film Growth	29
6. REFERENCES		31
7. LIST OF PUBLICATIONS		32

LIST OF FIGURES

		Page
Fig. 1	A comparison of thermal stress parameters of diamond and other laser materials	2
Fig. 2.	Schematic diagram of laser absorption and temperature rise in a host containing an isolated impurity	4
Fig. 3.	Variation of damage threshold with thermal conductivity of hosts containing impurities	5
Fig. 4.	Microwave plasma enhanced chemical vapor deposition system for diamond films	6
Fig. 5	(a) Diamond film on Si substrate for 16 hours	8
	(b) SEM photograph of diamond crystallites on a carbide substrate	9
Fig.6.	Diamond film grown at 1% methane concentration (a) on Si and (b) on tungsten carbide	10
Fig. 7.	Back surface of diamond film samples, after removing the Si substrate	11
Fig. 8	Raman spectrum of (a) the diamond film grown using 0.5% methane	12
	(b) a diamond film grown using 1% methane	13
	(c) a natural bulk diamond	13
Fig. 9.	Absorbance spectrum of a diamond film sample	14
Fig.10.	A two layer system of the analytical model for in-plane heat flow	16
Fig.11.	A block diagram of the experimental setup for diffusivity measurement	19
Fig.12.	A typical temperature profile obtained at four arbitrary time	20
Fig.13.	The phase of the thermal wave as a function of position	21
Fig.14.	Schematic diagram of the samples for LIDT measurement	24
Fig.15.	Schematic diagram of the differential reflectometer used in the damage threshold measurements	25
Fig.16	Differential reflectance vs. laser energy density for (a) 532 nm irradiation	26
	(b) 1064 nm irradiation	27
Fig.17	Micrographs of laser damage on (a) Si substrate, (b) diamond film on Si, and (c) diamond film window	28

LIST OF TABLES

		Page
Table 1	Comparison of important properties of diamond with other semiconductors	1
Table 2	Results of phase measurement	22
Table 3	Results of amplitude measurement	23
Table 4	Summary of results	23

1. INTRODUCTION

Diamond has many unique properties distinguishing it from other solid state materials. Included in these properties are its wide bandgap, high refractive index, high thermal conductivity, hardness and resistivity. Many important properties of diamond are shown in Table 1 and compared with those of other group IV elemental semiconductors and gallium arsenide.

Table 1

Comparison of important properties of diamond with other semiconductors

Properties	Ge	Si	GaAs	Diamond
Band Gap (eV)	0.66	1.12	1.43	5.45
Breakdown Field (V/cm)	~10^5	5x10^6	6x10^6	>10^7
Carrier Lifetime (s)	2x10^{-4}	2.5x10^{-3}	10^{-8}	~10^{-10}
Dielectric Constant	16	11.8	13.1	5.5
Electron Mobility (cm^2/V-s)	3900	1500	8500	1900
Electron Velocity (cm/s)	6x106	1x107	2x107	2.7x107
Hardness (Kg/mm^2)	780	103	600	104
Hole Mobility (cm^2/V-s)	1900	600	400	1600
Lattice Constant (Å)	5.64	5.43	5.65	3.57
Melting Point (^{o}C)	941	1420	1238	~3800
Refractive Index	5.6	3.4	3.6	2.4
Resistivity (Ohm-cm)	43	2.5x10^5	4x10^8	>10^{16}
Thermal Conductivity(W/cm-K)	0.64	1.45	0.46	20
Thermal Expansion Coefficient	5.5x10-6	2.6x10-6	5.9x10-6	8x10-7

It is obvious from Table 1, diamond is superior to other semiconductors in almost all properties listed above. These physical properties of diamond can be effectively exploited to develop electronic and optical devices which operate at high temperature and speed.[1-3] The wide bandgap and stable color centers in diamond have been used to make tunable solid state lasers.[4] With the progress achieved in gas phase deposition of diamond films, new applications of diamond films in laser optics are possible. High reflection and antireflection coatings currently used on optical elements in laser systems to optimize performance are often the weak links which limit the energy flux from a laser. Improvements in the laser damage threshold, E_D, of these films will significantly reduce design requirements as well as increase the transmitted laser power limits. A measure of the laser damage tolerance of a material called the thermal stress parameter, R_T, has been used as a figure of merit for evaluating materials.[5]

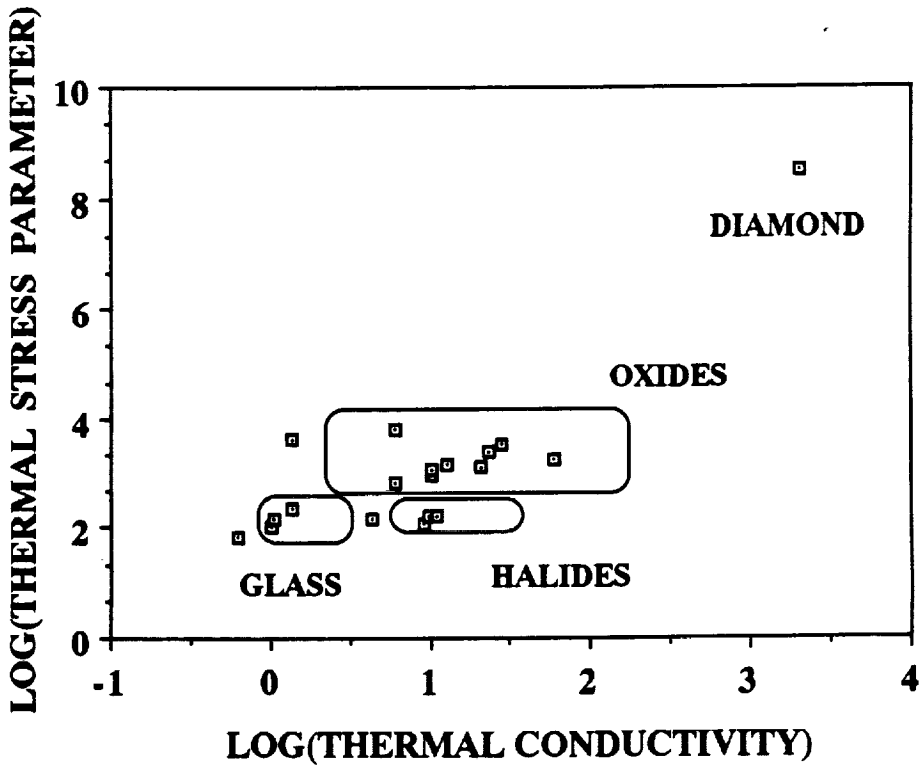

Figure 1. A comparison of thermal stress parameters of diamond and other laser materials.

This parameter is given by the relation

$$R_T = \sigma_f k(1-\nu)/\alpha E \qquad (1)$$

where σ_f is the tensile fracture strength of the material, k is its thermal conductivity, ν is its Poisson's ratio, α is its thermal expansion coefficient and E, its elastic modulus. High thermal stress parameters represent materials with high laser damage thresholds.

We have calculated R_T for diamond and several other common optical materials and display the results in Figure 1. The thermal conductivity and thermal stress resistance of similar materials cluster together in groups. The oxide group includes sapphire, spinel and commonly used garnets (YAG, GSGG). The halide group includes fluorides and chlorides of magnesium, calcium and lithium and the glass group includes phosphate and silicate glasses. Diamond, having a higher thermal conductivity and orders of magnitude higher thermal stress parameter, appears to be a good choice as a laser damage tolerant material. Hence diamond films may be used for a variety of optical coatings as well as optical windows.

2. LASER INDUCED DAMAGE

2.1 Dielectric Breakdown

If the damage is due to dielectric breakdown induced by the laser radiation, the laser power density, P_d, is related to the dielectric breakdown field, V_b, by the equation,

$$P_d = V_b^2 n/Z_o \qquad (2)$$

where n is the refractive index and Z_o is the impedance of free space. For bulk diamond, Equation (2) gives P_d = 600 GW/cm^2. For 10.6 μm laser radiation a threshold of 4 GW/cm^2 has been measured for bulk diamond.[6] In the case of thin films of high bandgap materials, the Forlani-Minnaja law[7] predicts $V_b \alpha d^{-1/2}$ where d is the film thickness. Therefore, diamond thin films should have a high breakdown field and a high laser damage threshold.

2.2 Damage due to Impurities

Thin films often contain impurities and inclusions which absorb the laser radiation; then the damage is caused by the thermal stress induced by laser heating. The temperature rise

of the host due to a spherical impurity absorbing radiation as shown in Fig. 2 is given by[8,9]

$$T_p=\frac{a^2QI}{k_p}\left[\frac{1}{3}\frac{k_p}{k_h}+\frac{1}{6}\left(1-\frac{r^2}{a^2}\right)-\frac{2ab}{r\pi}\int_0^{\alpha}\frac{e^{-\frac{y^2 t_p}{\gamma_1}}(\sin y - y\cos y)(\sin(ry/a))dy}{y^2\left[(c\sin y - y\cos y)+b^2y^2\sin^2 y\right]}\right] \quad (3)$$

k_p and k_h are the thermal conductivity of the impurity and host respectively, a is the radius of the impurity, Q is the absorption cross section, I is the laser intensity, t_p is the laser pulse duration and $b = [(k_p^2 D_h)/(k_h^2 D_p)]^{1/2}$,

$c = 1-(k_h/k_p)$ and $\gamma_1 = a^2/D_p$, where D_p and D_h are the thermal diffusivity of the impurity and the host. The above equation can be solved for the laser energy required for the melting points of the impurity or the host.

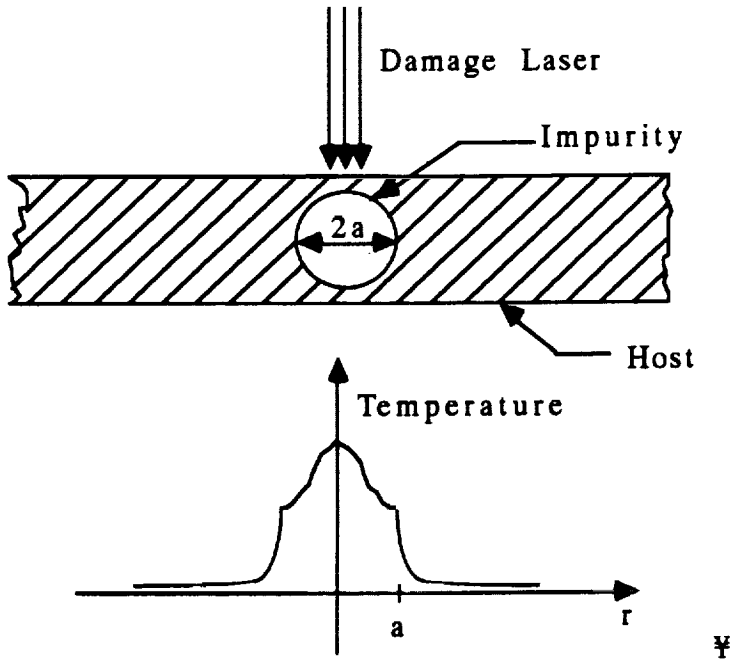

Figure 2. Schematic diagram of laser absorption and temperature rise in a host containing an isolated impurity.

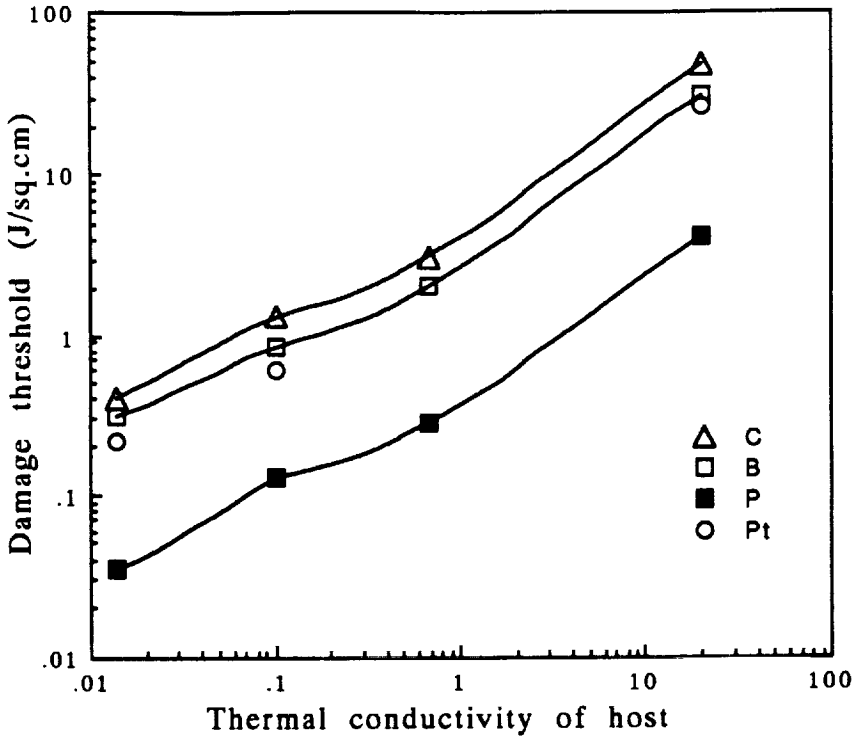

Figure 3. Variation of damage threshold with thermal conductivity of hosts containing impurities.

In Fig. 3 we show the variation of threshold energy density with k_h, required for breakdown at a = r, when various isolated impurities are present in the host. It is clear that the damage threshold of diamond is not severely affected by the impurities. Also for r >>a, the calculated value of E_d for diamond film was found to be a constant, independent of the thermal conductivity of the impurities.

In spite of the excellent properties discussed above, electronic and optical applications of diamond were limited due to the lack of large scale synthesis techniques. Bulk diamonds produced by high pressure-high temperature process are used as heat sinks and abrasives. However, this situation changed when Deryagin and Fedoseev[10,11] showed theoretically and experimentally that diamond could be synthesized in the metastable region at low temperature and low pressure using chemical vapor deposition process. The key to

the process is the control of super saturation of carbon on the substrate surface to enhance diamond growth and suppress graphite growth. This work has been verified by both Japanese and American researchers. Several modifications to this technique has been developed to grow diamond films on various substrates at varying conditions. These modified techniques include hot filament, acetelyne flame, and plasma enhanced chemical vapor deposition (PECVD)[12-16]. Among all the different techniques, PECVD process is a suitable method for producing uniform thin films on large area substrates.

3. DIAMOND FILM GROWTH AND CHARACTERIZATION

3.1 Microwave PECVD System

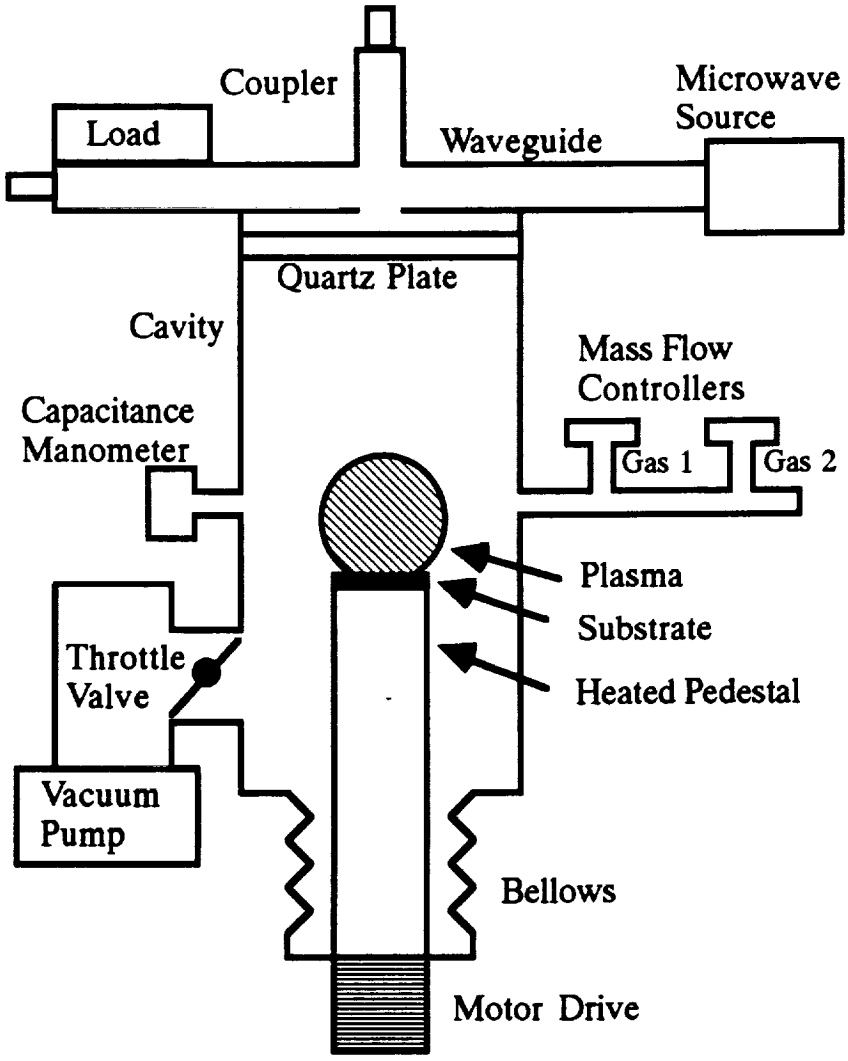

Fig. 4. Microwave plasma enhanced chemical vapor deposition system for diamond films.

The deposition system was assembled as shown schematically in Fig. 4. The microwave power can be varied from 300 to 1500 W. It is guided by the rectangular waveguide and fed to an axisymmetric coupler to produce a spherical plasma shape. The low pressure plasma chamber is separated from the waveguide at atmospheric pressure, using a quartz window. The chamber is evacuated using a turbo pumping system capable of a low vacuum to 10^{-5} torr. An automatic pressure control unit maintains the working pressure at a fixed value up to 20 torr. The substrate is placed on a graphite stage which is heated by an RF induction heater and a temperature control assembly from room temperature to 1100 ^{o}C. Two separate mass flow controllers are used to maintain H_2 and CH_4 flow in to the deposition system. The system is tested for microwave power leakage below the safe level. The system is also fitted with interlocks for water flow, over temperature and gas leaks. Trial experiments were conducted for the proper operation of the system and conditions were established to grow diamond films on silicon substrates.

3.2 Substrate Preparation

It was found that the surface texture plays an important role in the nucleation of diamond film. Preferential nucleation occurs on scratch marks on the substrate. To increase the nucleation density, the substrates were abraded with 0.1 μm diamond paste. Si wafers were used as substrates for most of the growth studies. Tungsten carbide substrates were also used to study the differences in nucleation. In each case the substrate was cleaned in acid and base solutions and rinsed in ethanol and blow-dried.

3.3 Diamond Film Growth

Experiments were conducted to grow diamond film on the samples. The substrate temperature was varied from 900 to 1100 ^{o}C; the methane content in hydrogen was varied from 0.1 to 1.0 % in the gas mixture and the gas pressure from 1 to 20 torr. These process parameters were varied systematically and the samples were analyzed using an SEM and Raman spectroscopy. The most significant parameter for the growth of diamond film with

well defined facets was found to be the percentage of methane content in hydrogen. Under all the operating conditions, films could be grown on all the substrates the films were stable on Si and carbide substrates.

3.4 Diamond Growth using 0.5% CH_4

Fig. 5(a) shows the SEM photograph of a diamond film grown on a Si substrate for a 16 hours growth time. The growth rate is approximately 1μm per hour for deposition carried out using 1000 W of microwave power at 20 torr. The substrate was maintained at 900°C. The film is continuous and polycrystalline. This is due to a high density of nucleation on the Si substrate.

Fig. 5(a). Diamond film on Si substrate for 16 hours.

Under the same growth conditions the film grown on a carbide substrate is shown in Fig. 5(b). The film is not fully continuous yet; instead, well defined facets of the diamond crystallites are visible. More importantly, the crystallites are of fairly uniform size which

indicates that all of them were nucleated simultaneously and very few new nucleation centers were produced on the substrate surface during the subsequent growth time. On further growth, the crystallites would coalesce to form a continuous film.

Fig. 5(b). SEM photograph of diamond crystallites on a carbide substrate.

Secondary growth on the crystallites are clearly visible while there is no evidence for new nucleation on the carbide substrate surface. Hence it is reasonable to assume that the film growth is mainly due to diamond growth on diamond crystallites to form a continuous film. Therefore it is important to have high density of nucleation to begin with on the substrate. For a 12 μm film to be continuous, the minimum nucleation density must be of the order 10^6 cm^{-2}. As seen in Fig. 5(a), it is easy to achieve this high nucleation density on a Si substrate. We estimate the nucleation density in Fig. 5(b) is around 10^5 cm^{-2}. To achieve a thinner, continuous film on a carbide substrate, a higher nucleation density is required. For other optical applications, the film thickness will be about a 1μm and therefore, the nucleation density must be higher than 10^8 cm^{-2}.

3.5 Diamond Film Growth using 1% CH_4

Under identical conditions given above, for the methane concentration of 1%, a continuous film is obtained at 22 hours of deposition. Fig. 6(a) and (b) show the SEM photographs of these samples on Si and WC substrate respectively.

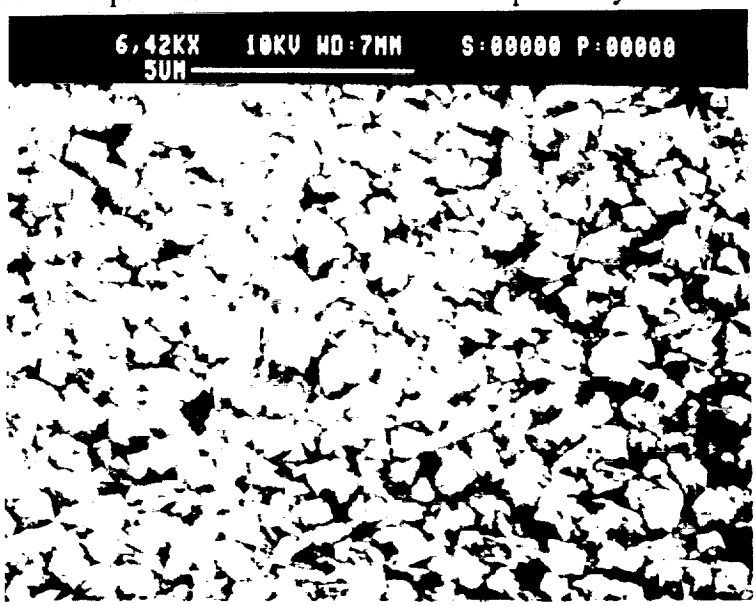

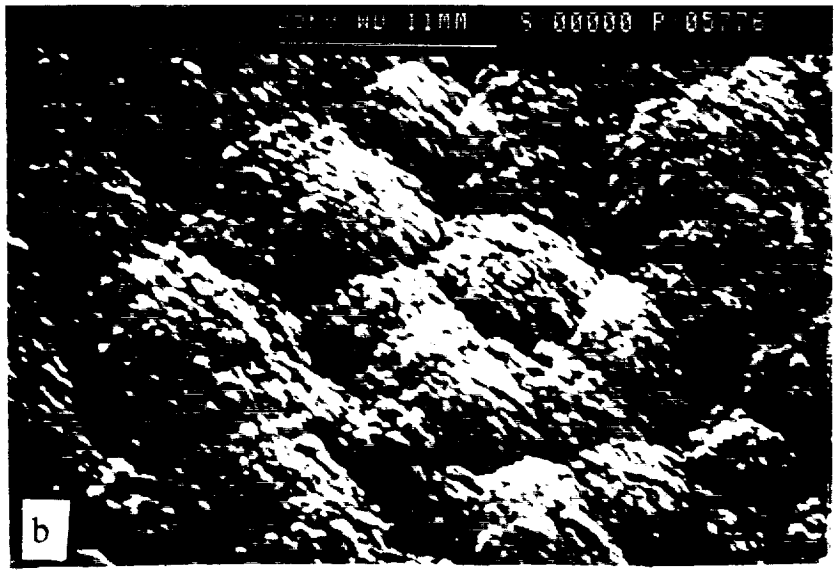

Fig. 6. Diamond film grown at 1% methane concentration.
(a) on Si and (b) on tungsten carbide.

The films contain both diamond and graphite. The film topography is smooth. The physical properties of these films will be inferior to those of the samples shown in Fig. 5, due to the presence of graphite. All the diamond film samples grown were polycrystalline. The front surface was always faceted whereas the back surface which was in contact with the substrate (etched-back) was smoother than the front as shown in the SEM photograph (Fig. 7). The back surface of the film replicates the substrate surface, which might be useful to produce smooth diamond surfaces for optical application.

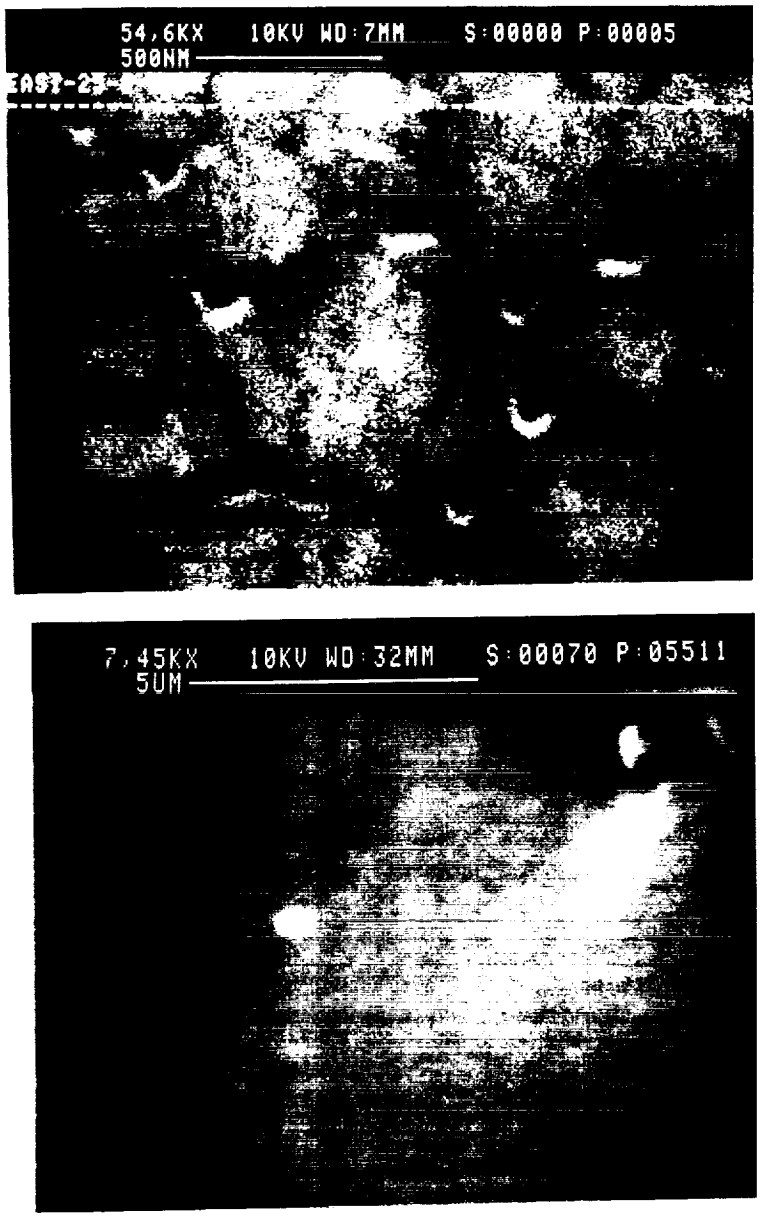

Fig. 7. Back surface of two diamond film samples, after removing the Si substrate.

3.6 Diamond Film Characterization

3.7 Raman Spectroscopy

Raman spectroscopy is one of the characterization techniques commonly used for diamond film to assess the nature of the chemical bonding state of carbon. The Raman spectra of the sample films grown using 0.5 and 1% methane concentration are shown in Fig. 8(a) & (b).

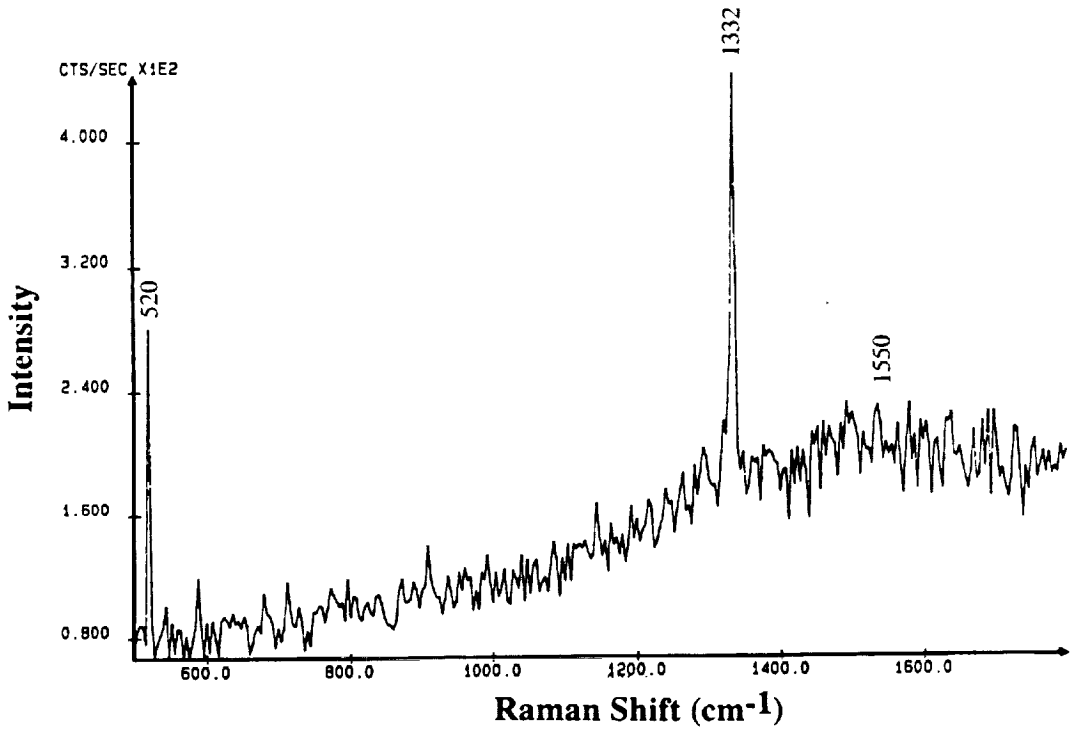

Fig. 8(a). Raman spectrum of the diamond film grown using 0.5% methane.

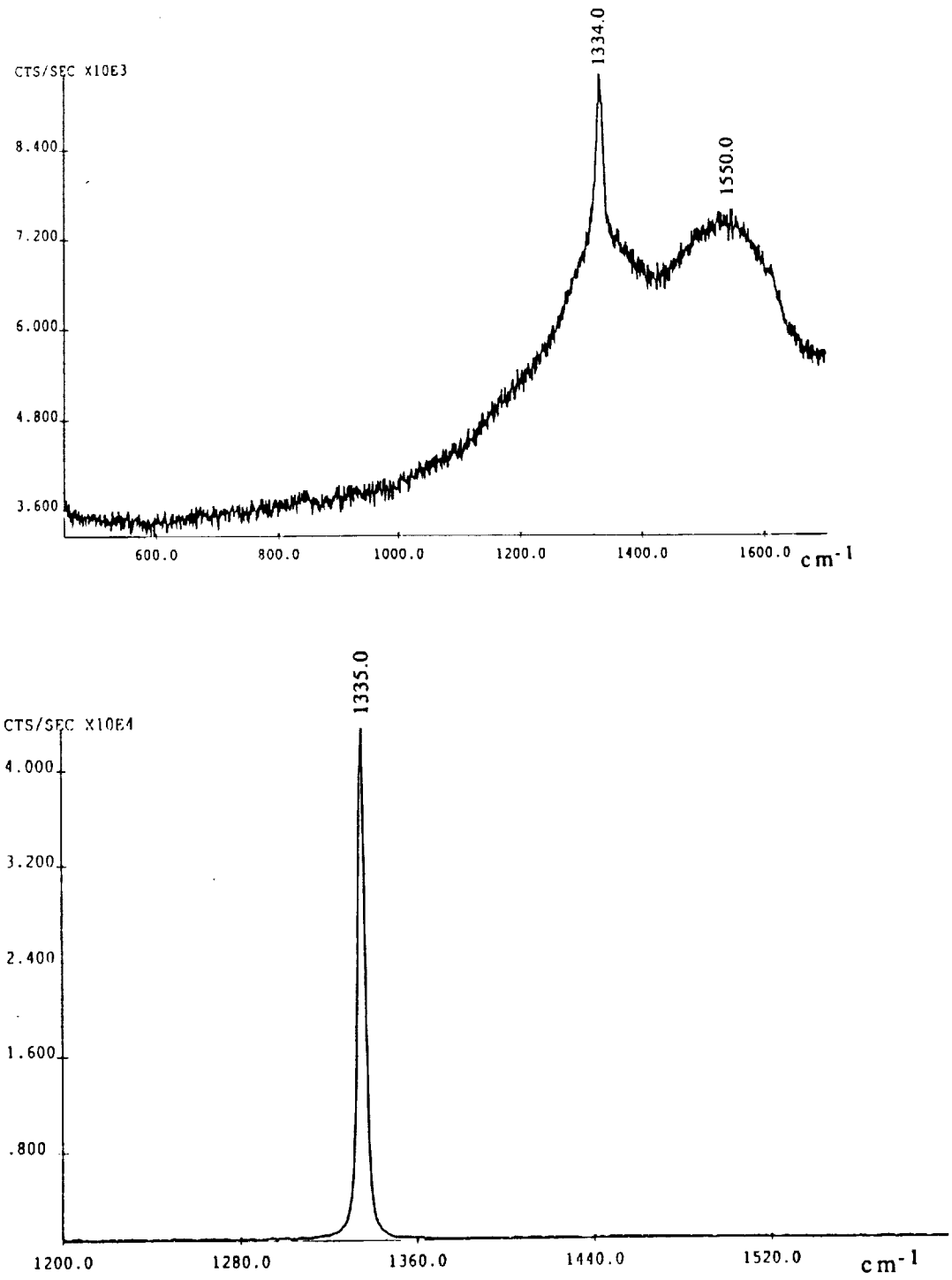

Fig. 8. Raman spectra of (b) a diamond film grown using 1% methane (c) a natural bulk diamond

All the diamond films showed characteristic first order Raman spectral line around 1332 cm^{-1}, which may be compared with the spectrum shown in Fig. 8(c) for a natural bulk diamond. The significant difference between the spectra is a broad fluorescence background centered around 1550 cm^{-1} for the diamond films, which is an indication of the presence of sp^2 bonding due to graphitic carbon in diamond film. Since the sensitivity of Raman scattering for sp^2 bonded carbon is almost two orders of magnitude higher compared to that of sp^3 bonded carbon, we conclude that the films were predominantly diamond. The line at 520 cm^{-1} is due to the silicon substrate. The sp^2 content in the film grown using 0.5% methane concentration is considerably lower than that of the 1% case as can be seen by comparing the sp^2 signals in Fig. 8 (a) & (b).

3.8 Absorbance Spectrum of Diamond Film

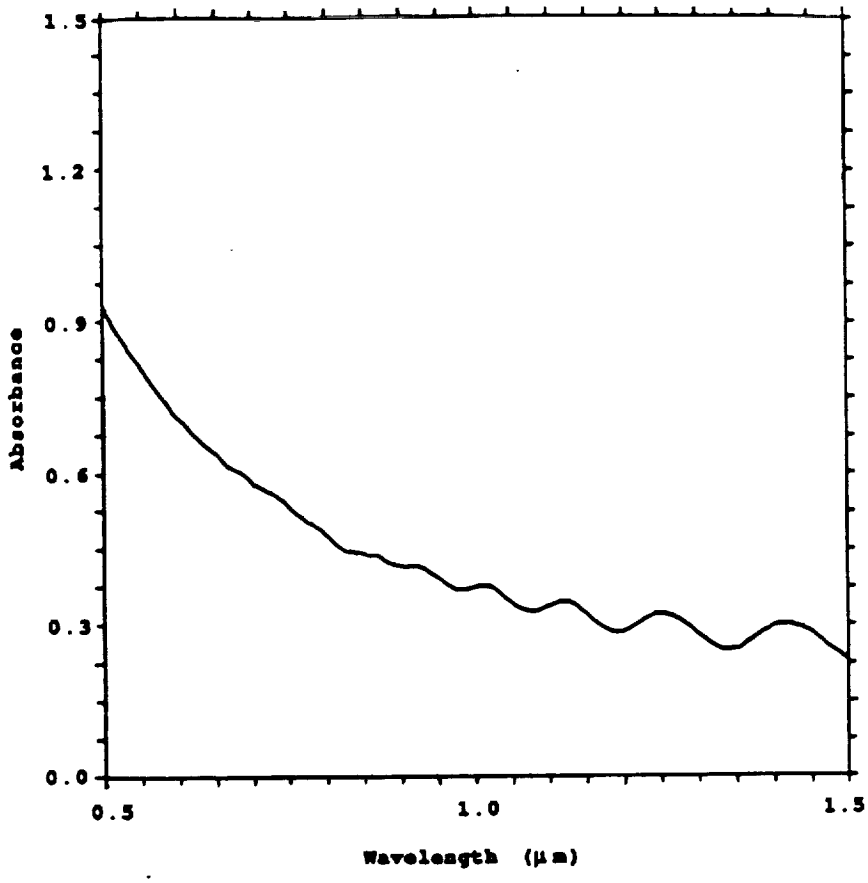

Fig. 9. Absorbance spectrum of a diamond film sample.

The absorbance spectrum of diamond films was measured using a Perkin Elmer spectrophotometer and is displayed in Fig.9, for the wavelength range from 500 to 1500 nm. Interference effects due to the film (1.87 μm) can be clearly seen. No correction for Fresnel reflectance from the film has been made in the absorbance spectrum shown. Absorption of the film increases towards shorter wavelengths. The absorption coefficients at 532 and 1064 nm, derived from Fig. 9 by applying the corrections for reflectance are $\alpha_{532} = 3.93 \times 10^3\ cm^{-1}$ and $\alpha_{1064} = 1.20 \times 10^3\ cm^{-1}$. These high values are due to the graphitic content and defects in the diamond film and are higher than the absorption coefficients of other optical thin film materials by three orders of magnitude.

3.9 Thermal Diffusivity of Diamond Films

Thermal diffusivity of diamond film is critical for its performance in many applications. Diamond films have a high value of thermal shock resistance parameter due to the large value of thermal conductivity. This leads to a high threshold for laser induced damage. Likewise, the damage threshold of diamond films is not affected by the presence of isolated impurities because of its high thermal diffusivity. Theoretical studies on the effect of an intermediate layer of diamond film between a metal film and a substrate have shown that a diamond film of about 1μm will be sufficient to reduce the temperature of the metal film induced by x-ray pulses of nanosecond duration [17]. Also, it has been shown that diamond is able to withstand the high thermal loads due to the internal photon flux in a free electron laser cavity[18]. In addition to being a good thermal conductor, diamond can also be used to make electronic devices operating at high temperature. In many of these applications diamond thin films are used. Defining the limits of the applicability of diamond films requires a measurement of their thermal diffusivity. The high thermal diffusivity and thin film geometry make standard thermal analysis inadequate for experimental determination. For example, an experimental method based on radiation heat transfer and radiation thermometry has been reported to measure the thermal conductivity of diamond films[19]. Here, the substrate was removed by etching and the unsupported film was too fragile to mount on a heated holder. The sample was coated with a black paint whose emissivity was

assumed to be unity. A laser pulse technique was developed to measure the effective in-plane (face parallel) diffusivity of diamond film deposited on a substrate. The substrate need not be removed. The phase and amplitude variation of the in-plane thermal wave was measured which is independent of the emissivity of the black paint.

3.10 Analysis

An analytical model describing in-plane heat flow in a two layered system was developed to reduce the measured thermal diffusivity of the sample to a thermal diffusivity for the diamond film. Two dimensional heat flow in each of the homogeneous isotropic layers shown in Fig.10, is described by,

$$\nabla^2 T_n(x,y,t) - \frac{1}{\alpha_n} \frac{\partial T_n(x,y,t)}{\partial t} = 0 \qquad (5)$$

where $T_n(x,y,t)$ and α_n are the temperature and thermal diffusivity of the respective solids.

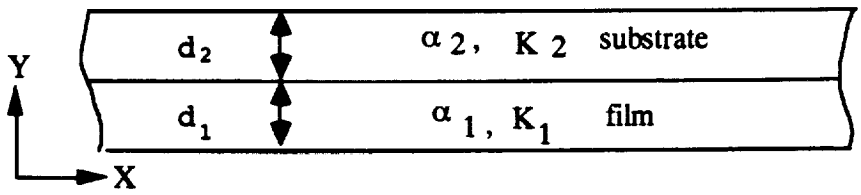

Fig. 10. A two layer system of the analytical model for in-plane heat flow.

Assuming no exterior surface heat flow of the two layer system (i.e. convection and radiation losses are negligible), a solution for a thermal wave excited by a periodic source and propagating in the x direction is

$$T_1(x,y,t) = A\, e^{j(k\,x - t\,\omega)} \cos\left[y \left(-k^2 + \frac{(j*\omega)}{\alpha_1} \right)^{1/2} \right] \qquad (6),$$

for the first layer and

$$T_2(x,y,t) = B\, e^{j(k\,x - t\,\omega)} \cos\left[(d_1 + d_2 - y)\left(-k^2 + \frac{(j*\omega)}{\alpha_2}\right)^{1/2}\right] \tag{7},$$

for the second layer, where d_1 and d_2 are the layer thicknesses, k is the propagation constant and ω is the angular frequency of the excitation.

At the interface of the two layers the temperature and flow are continuous which can be expressed as

$$T_1(x,d_1,t) = T_2(x,d_2,t) \tag{8},$$

and

$$K_1 \frac{\partial T_1(x,y,t)}{\partial y} = K_2 \frac{\partial T_2(x,y,t)}{\partial y} \tag{9}$$

for $y = d_1$, where K_1 and K_2 are the thermal conductivities of the two layers.
Equations (6), (7), (8) and (5) can be expressed in a matrix form as

$$\begin{bmatrix} \cos(s_1) & \cos(s_2) \\ K_1 \sin(s_1)\left(-k^2 + j\,\omega/\alpha_1\right)^{1/2} & -K_2 \sin(s_2)\left(-k^2 + j\,\omega/\alpha_2\right)^{1/2} \end{bmatrix} \begin{bmatrix} A \\ B \end{bmatrix} = 0 \tag{10}$$

where s_1 and s_2 are defined as

$$s_1 = d_1\left(-k^2 + \frac{j\,\omega}{\alpha_1}\right)^{1/2} \tag{11},$$

and

$$s_2 = d_2 \left(-k^2 + \frac{j\,\omega}{\alpha_2}\right)^{1/2} \qquad (12).$$

Nontrivial solutions for A and B exist when the determinant of the matrix in equation (10) is zero, which can be expressed as the transcendental equation,

$$K_1 \cos(s_2) \sin(s_1) \left(-k^2 + \frac{j\,\omega}{\alpha_1}\right)^{1/2} + K_2 \cos(s_1) \sin(s_2) \left(-k^2 + \frac{j\,\omega}{\alpha_2}\right)^{1/2} = 0 \qquad (13).$$

For small s_1 and s_2, $d_1(\omega/\alpha_1)^{1/2}$ and $d_2(\omega/\alpha_2)^{1/2}$ are much less than 1. This assumption is especially valid in the case of diamond and silicon for low frequency thermal excitation. The solution for k can be written as

$$k = \pm \left\{ \frac{j\omega(\alpha_2 K_1 d_1 + \alpha_1 K_2 d_2)}{\alpha_1 \alpha_2 (K_1 d_1 + K_2 d_2)} \right\} \qquad (14).$$

By comparison with heat propagation in a single layer, the propagation constant can be written in the form

$$k = \pm \left(\frac{j\,\omega}{\alpha_e}\right)^{1/2} \qquad (15),$$

where α_e is an effective in-plane diffusivity, given by the expression

$$\alpha_e = \frac{\alpha_1\,\alpha_2\,(K_1\,d_1 + K_2\,d_2)}{\alpha_2\,K_1\,d_1 + \alpha_1\,K_2\,d_2} \qquad (16)$$

The thermal conductivity of the sample is related to its thermal diffusivity by the expression

$$k = c\rho\,\alpha \qquad (17)$$

where c is the specific heat and ρ is the density. Using the values of specific heat and density of layer 1, the thermal properties of the second layer, the thickness of the layers and the measured effective diffusivity of the double layer system, the diffusivity of layer 1 can be found from

$$\alpha_1 = \frac{c_1\rho_1\alpha_2\alpha_e d_1 - \alpha_2 K_2 d_2 + \alpha_e K_2 d_2}{c_1\rho_1\alpha_2 d_1} \qquad (18).$$

3.11 Thermal Diffusivity Measurement

To measure the thermal diffusivity of the sample, a portion of the samples was heated and the time dependence of the surface temperature was measured. A block diagram of the experimental setup used for these measurements is shown in Fig. 11.

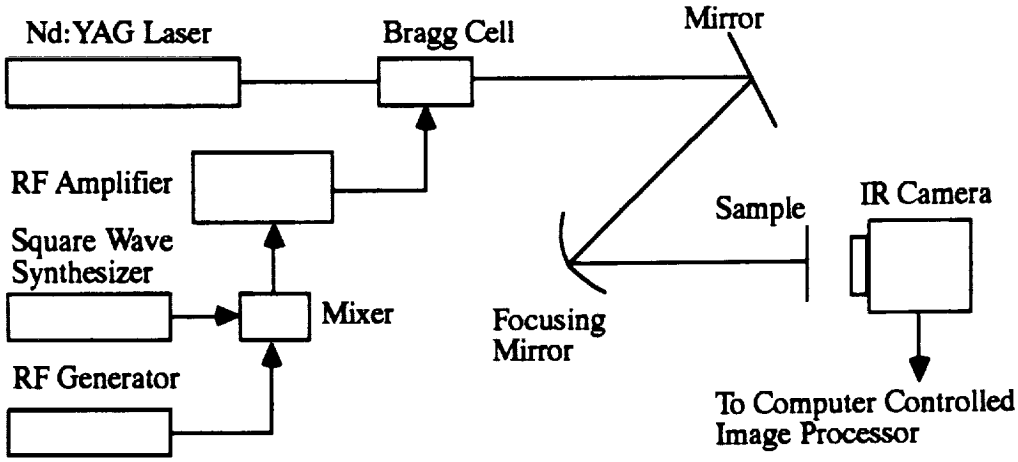

Fig. 11. A block diagram of the experimental setup for diffusivity measurement.

The periodic heat source was the output of a 20 watt, 1.064 μm Nd:YAG laser. The output was focused to a spot less than 1 mm in diameter on the sample. The output of the laser was modulated at a select frequency, by exciting a Bragg cell, which was within the laser cavity. The power output of the laser was adjusted to fix the sample temperature within 25 to 35 °C. To measure the spatial temperature distribution of the sample, an 8-12 μm infrared camera with a spatial resolution of better than 1 mm was used. The camera was positioned with its axis perpendicular to the sample.

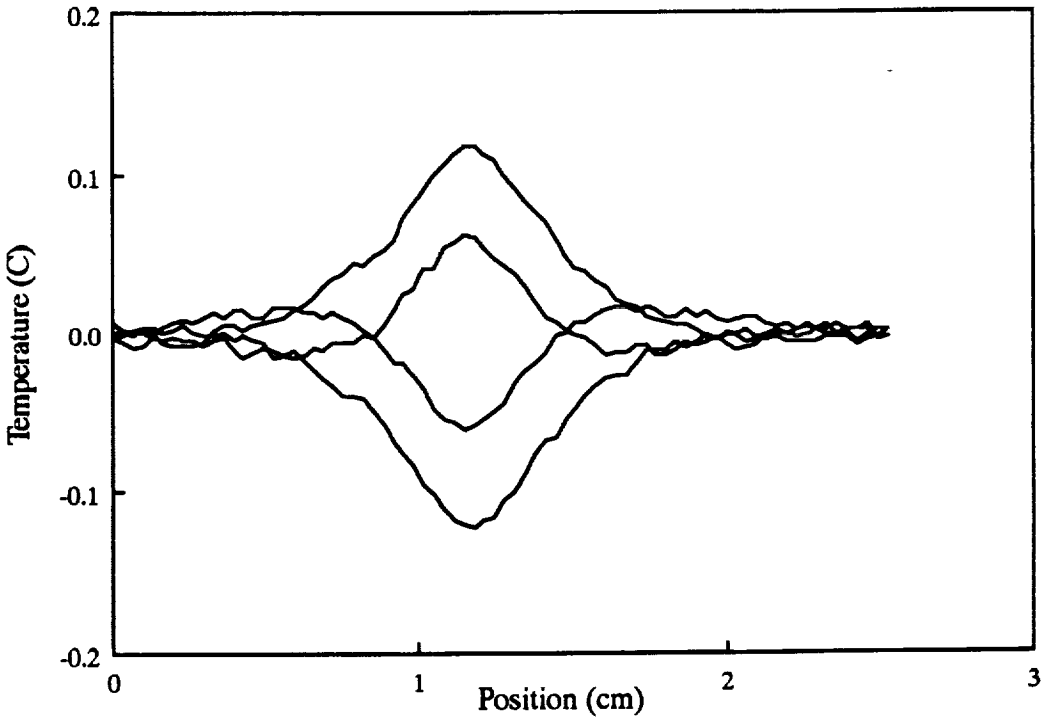

Fig. 12. A typical temperature profile obtained at four arbitrary times.

Temperature measurements were performed in a mode where the camera scanned a single horizontal line that passed through the center of the sample and the heating zone. The camera output of the temperature images was in a standard video format (RS330). An image processor was used to digitize 128 successive images. Each image was compressed to a single temperature profile across the sample resulting in sampling of temperature over 1/30 of a second. The resulting temperature profiles as a function of time were then stored for off-line processing. For the work presented here, data were collected using symmetric, periodic heating at 2.812, 3.281 and 3.750 Hz. Typical temperature profiles obtained at four different times are shown in Fig. 12. For a cyclic heating source, the diffusivity of the sample can be calculated from the spatial phase and amplitude dependence sufficiently far from the source.

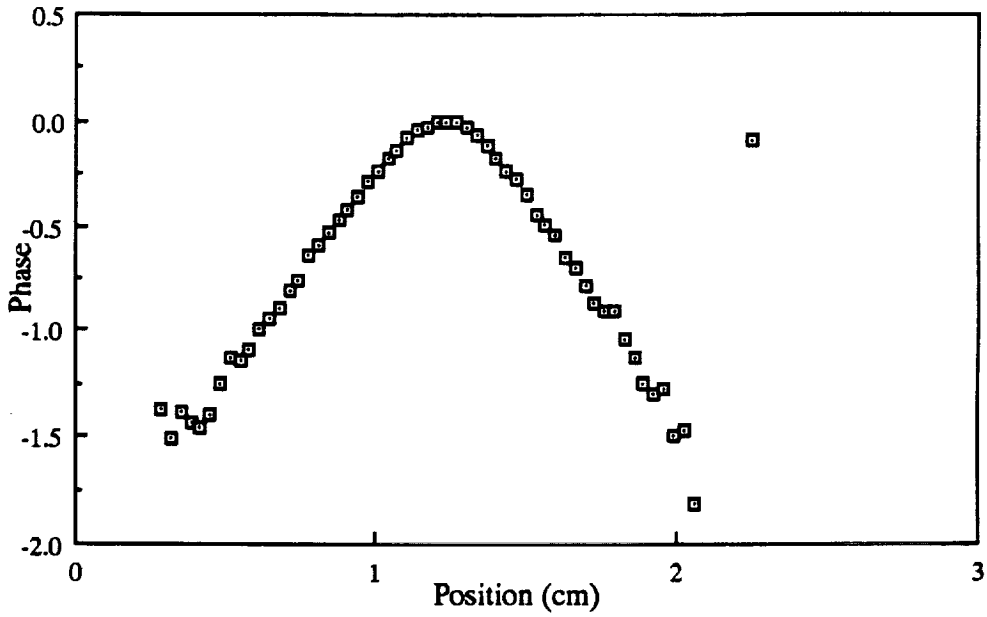

Fig. 13. The phase of the thermal wave as a function of position.

To obtain the phase and amplitude of the signal at each point on the sample, a complex fourier transform at each point was performed. The phase was determined from the arctangent of the imaginary part of the fourier transform divided by the real part. The calculated phase as a function of position is shown in Fig. 13. As can be seen in this figure a portion of the phase away from the point of excitation, is linearly dependent on position. The effective diffusivity α_e can be calculated from the slope of the phase in this region using the equation,

$$\alpha_e = \frac{\pi f}{s^2} \qquad (19),$$

where s is the slope of the phase and f is the excitation frequency. Using the same measurement technique, the diffusivity of a bare silicon substrate was found to be $1.04 \pm .02$ cm^2/sec, which is in reasonable agreement with results from other method of

measurements[20]. Using equation (19) and the measured slopes, the effective diffusivity was calculated for each sample at each frequency, which is shown in Table 2 for two samples.

Table 2

Results of phase measurement

Frequency (Hz)	Slope of phase (cm^{-1})		Effective diffusivity ($cm^2\ sec^{-1}$)	
	16 μm film	32 μm film	16 μm film	32 μm film
2.812	2.45	2.08	1.47	2.04
3.281	2.56	2.41	1.57	1.77
3.750	2.80	2.59	1.50	1.76

From these measurements and equation (18), the diffusivity of the diamond film is found to be 8.10± .32 cm^2/sec for the 16 μm thick film and 7.57±.7 cm^2/sec for the 32 μm thick film. Using equation (17), thermal conductivity is found to be 14.68 and 13.70 W/cmK respectively. These values are better than that of type Ia natural diamond. It has been shown[19] that the value of thermal conductivity of diamond films depends strongly on the presence of graphitic carbon in the films. A small amount of sp^2 bonded carbon was detected in our films as seen from the Raman spectrum shown in Fig. 8(a). However, its effect on thermal diffusivity can not be judged from the present experimental results.

The values of effective diffusivity of the composite diamond and silicon can also be determined using the amplitude method. A least square fit of the spacial dependence of the measured amplitude with the amplitude of the modified Bessel function[21],

$$A K_0\{(j\omega/\alpha_e)^{1/2} r\} \qquad (20)$$

was carried out,where r is the distance from the center of the laser heating and A is a normalization factor. Table 3 shows the effective diffusivity determined by this method at three different frequencies used for the measurement. The average effective diffusivity values are 1.47 ± .03 and 1.83 ± .10 yielding thermal diffusivity values of 7.46 ± .90 and 7.33 ± .70 cm^2/ sec respectively for the two samples and the calculated thermal

conductivity values are 13.50 and 13.28 W/cmK. These are better than that of type 1a natural diamond.

Table 3

Results of amplitude measurements

Frequency (Hz)	Effective diffusivity ($cm^2\ sec^{-1}$)	
	16 μm film	32 μm film
2.812	1.44	1.90
3.281	1.49	1.71
3.750	1.50	1.91

Table 4

Summary of the Results

Method	Effective diffusivity of composite (sq.cm/sec)	Diffusivity of diamond film (sq.cm/sec)	Thermal conductivity of diamond film (W/cmK)	Diamond film thickness (μ m)
Phase	1.51	8.10	14.68	16
	1.86	7.57	13.70	32
Amplitude	1.47	7.46	13.50	16
	1.83	7.33	13.28	32

From the summary of results shown in Table 4, it can be seen that excellent agreement has been obtained for the thermal diffusivity values measured using the two methods.

4. LASER INDUCED DAMAGE THRESHOLD MEASUREMENT

Silicon wafers were used as substrates. Free-standing diamond film windows were produced by etching holes in the substrate. Three different types of samples as shown in Fig.14, were used for the LIDT measurement.

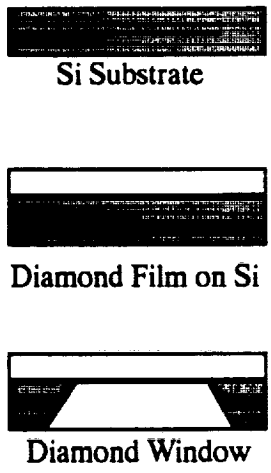

Fig. 14. Schematic diagram of the samples for LIDT measurement.

Laser damage on the samples was induced by varying the energy from 1 to 100 mJ from a 1064 nm Nd:YAG laser with a pulse duration of 20 ns. Silicon, diamond film on silicon and diamond film windows were used as samples. The diameter of the laser spot at the impact point was measured using an array detector. The laser damage threshold was measured using the setup shown schematically in Fig. 15. The sample was mounted on an X-Y-Z microposition stage. A He-Ne laser was used as a probe to measure the reflectance of the surface.The reflection from an undamaged portion of the surface was detected and fed to the lock-in amplifier along with the reference signal to obtain a null point. The probe was then positioned on the damaged spot and the intensity of the reflected beam was measured. A deviation from the null condition occurred when the reflected intensity changed, due to absorption and scattering from the damaged spot. The deviation was measured as a function of laser damage energy. The damage on the films was also

confirmed by using a low power optical microscope. The experimental set-up could be easily modified to detect the scattered light by blocking the specular reflection.

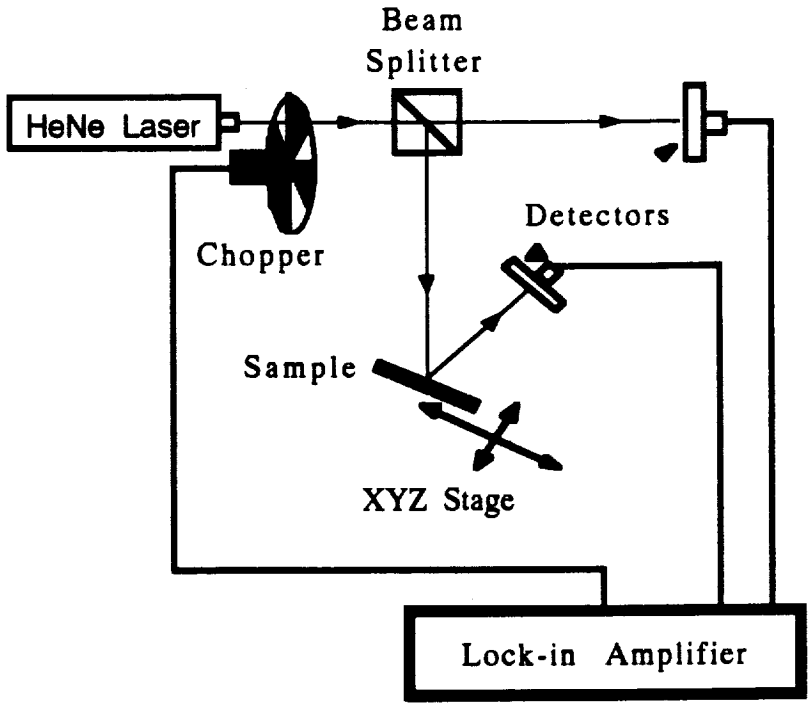

Fig. 15. Schematic diagram of the differential reflectometer used in the damage threshold measurements.

In Fig. 16a and b we show the results of laser damage on silicon substrate, diamond film on silicon and diamond film windows for 532 and 1064 nm laser radiation respectively. The output signal from the lock-in amplifier is plotted against the laser energy. The damage threshold of silicon was measured to be 5.3 J/cm^2 (265 MW/cm^2) for 1064 nm and 2.1 J/cm^2 (105 MW/cm^2) for 532 nm laser pulses. These are within the range of values reported for silicon.[22] The irradiated spots were also examined using a low power optical microscope for laser induced damage and the threshold energy agreed with that determined by the reflectance technique. The absorption coefficients of silicon at these wavelengths are high and energy transfer by resonant surface plasmons has been considered as a damage mechanism.[23] The measured damage thresholds for a silicon substrate coated with a 1.87 μm diamond film are 3.65 J/cm^2 (182 MW/cm^2) at 532 nm

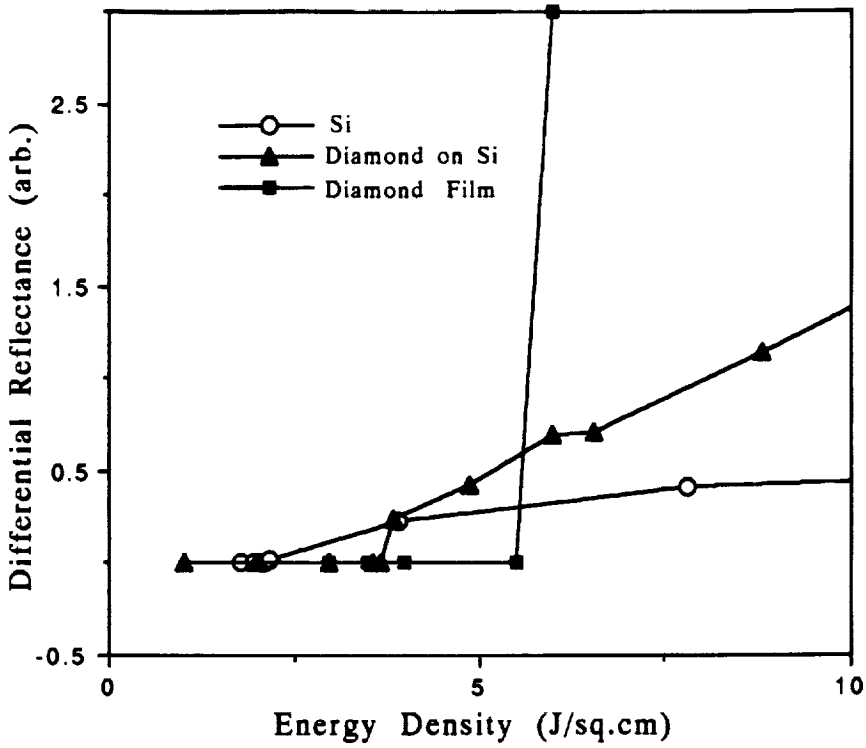

Fig. 16 (a). Differential reflectance vs. laser energy density of 532 nm irradiation.

and 14.4 J/cm^2 (720 MW/cm^2) at 1064 nm. The reflectance of silicon substrate is about 30% and the 1.87 μm diamond film corresponds to approximately an equivalent optical thickness of quarter wavelength at 532 nm. For this film-substrate combination, the reflectance is reduced to approximately 8%. Assuming the laser damage threshold of diamond to be higher than silicon, it is reasonable to expect a threshold of 1.6 J/cm^2 for this film-substrate combination, if the damage occurs mainly at the substrate. The measured damage threshold at 532 nm is higher than that of the substrate, showing the effectiveness of a diamond film for laser hardening. In the case of 1064 nm laser radiation, the same diamond film has an optical thickness of non-quarter wavelength; hence the reflectance of the film-substrate combination is between 8 and 30%. Moreover, for a non-quarter wavelength film the maximum electric field due to the laser radiation will be within the film rather than at the interface. Such a design has been shown to be beneficial in

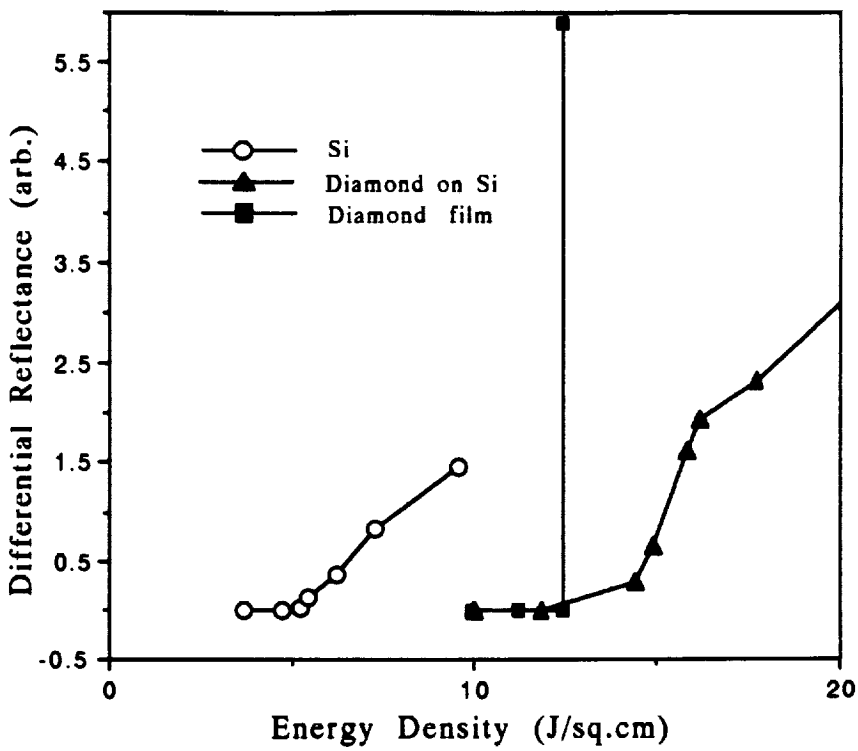

Fig. 16(b). Differential reflectance vs. laser energy density of 1064 nm irradiation.

achieving a high damage threshold for optical coatings.[24] The high damage threshold of 14.4 J/cm^2 at 1064 nm obtained for the film-substrate combination is an indication that diamond film will be useful for a variety of optical coating applications involving high power lasers.

For a diamond film thickness of 1.87 μm, the laser damage thresholds at 532 and 1064 nm were found to be 6.0 J/cm^2 (300 MW/cm^2) and 12.4 J/cm^2 (620 MW/cm^2) respectively. These values are substantially higher than those measured for the silicon substrate. Thus, the low damage threshold of the film-substrate combination discussed above for 532 nm is not due to the diamond film. However, the damage threshold measured for free-standing diamond film is lower than theoretically predicted value. Since the films have high absorption coefficient due to sp^2 bonded carbon the contribution from these impurities will be substantial in determining the damage threshold. However, the damage threshold may be further improved by optimizing deposition conditions.

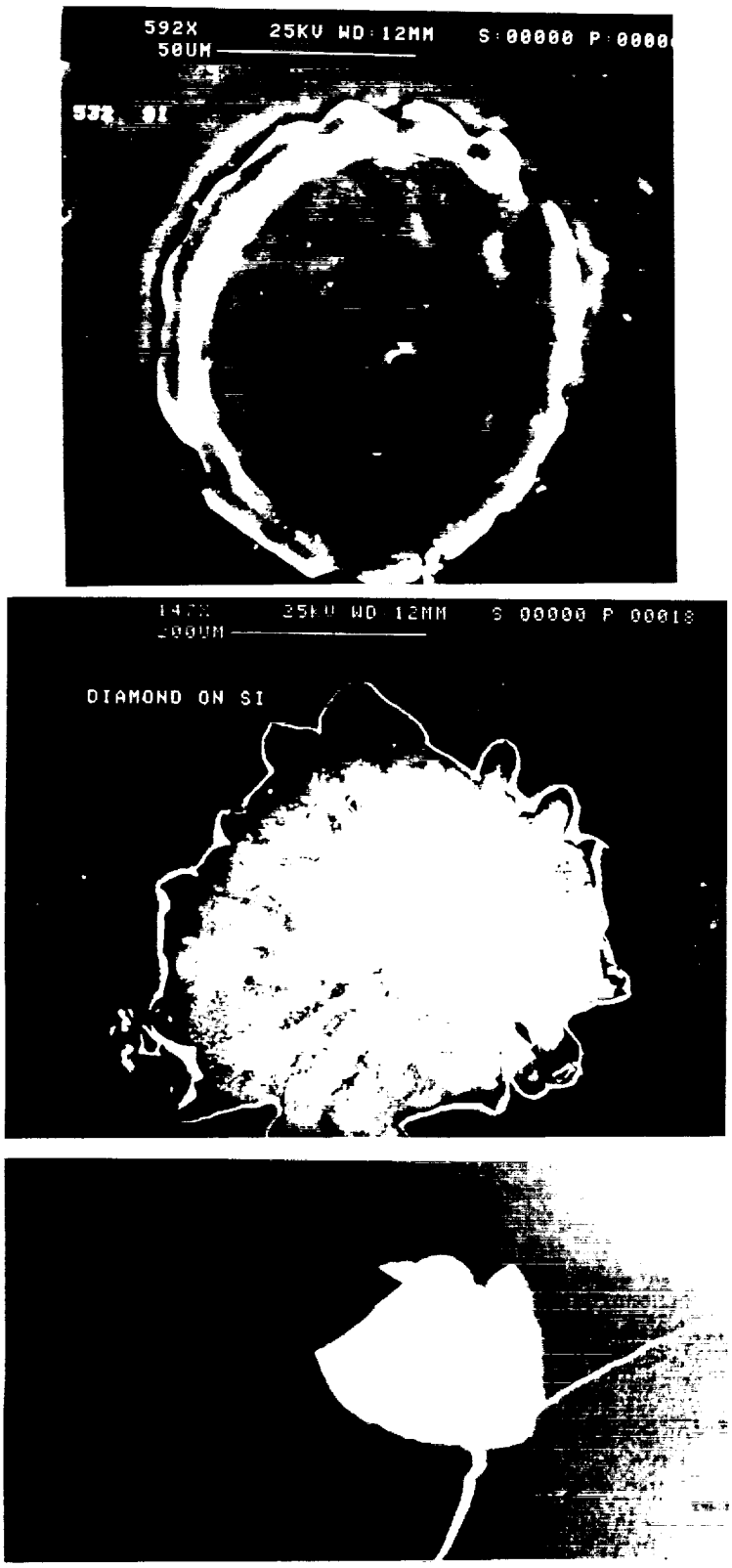

Fig. 17 Micrographs of laser damage on

(a) Si substrate, (b) diamond film on Si, and (c) diamond film window.

In Fig. 17 we show the SEM photographs of laser damage on various samples. There is an obvious difference in the nature of damage on silicon substrate and on film-substrate combination. Surface melting is visible on silicon whereas the damage on the latter appears to be due to dielectric breakdown. The diamond films developed cracks during laser damage suggesting that the film stress may influence the damage threshold.

5. FURTHER RESEARCH

5.1 High Density Nucleation

A high density of nucleation will be required to produce a continuous film. The adhesion of such a film on the substrate will be superior to that of films coalesced by growth on crystallites. More work on the surface preparation of the substrate is necessary to arrive at the optimum condition for high density nucleation.

5.2 Low Temperature Growth

The properties of the substrates may be adversely affected by the high temperature of diamond film growth. This may be true for the optical surfaces as well. In presence of oxygen, the growth temperature can be reduced as low as 450 ^{o}C. Addition of oxygen also improves the quality of the diamond films by etching away the graphitic carbon produced during growth. Hence diamond growth studies at a low temperature and in presence of oxygen will be useful.

6. REFERENCES

1. M. W. Geis, D. D. Rathman, D. J. Ehrlich, R. A. Murphy and W. T. Lindley, "High temperature point contact transistors and Schottky diodes formed on synthetic boron doped diamond", IEEE Electron Device Lett., EDL-8(8), 341-343 (1987).
2. J. F. Prins, "Bipolar transistor action in ion implanted diamond", Appl. Phys. Lett. 41(10), 950-952 (1982).
3. P. S. Panchhi and H. M. Van Driel, "Picosecond optoelectronic switching in insulating diamond", IEEE J. Quantum Electron. QE-22 (1), 101-107 (1986).
4. S. C. Rand and L. G. DeShazer, "Visible color-center laser in diamond", Optics Lett. 10(10), 481-483 (1985).
5. W. F. Krupke, M. D. Shinn, J. E. Marion, J. A. Caird and S. E. Stokowski, "Spectroscopic, optical and thermal properties of neodymium- and chromium-doped GSGG," J. Opt. Soc. Am. B, 3(1), 102-114 (1986).
6. R. M. Wood, Laser Damage in Optical Materials, Adam Hilger, Bristol (1986).
7. F. Forlani and N. Minnaja, "Thickness influence in breakdown phenomena of thin dielectric films", Phys. Stat. Sol. 4, 311-324(1964).
8. H. Goldenberg and J. C. Tranter, "Heat flow in an infinite medium heated by a sphere," Brit. J. Appl. Phys. 3, 296-298(1952).
9. T. W. Walker, A. Vaidyanathan, A. H. Guenther and P. Nielsen,"Impurity breakdown model in thin films," in Laser Induced Damage in Optical Materials: 1982, H. E. et.al. ed. National Bureau of Standartds, 479-496(1984).
10. D. V. Fedoseev, V. P. Varnin and B. V. Deryagin, "Synthesis of diamond in its Thermodynamic Metastability Region", Russian Chem. Rev., 53, 435-444(1984).
11. B. V. Spitsyn, L. L. Bouilov and B. V. Derjaguin, "Vapor growth of diamond on diamond and other surfaces", J. Crystal Growth, 52, 219-226(1981).
12. S. Matsumoto, Y. Sato, M. Tsutsumi and N. Setaka, "Growth of diamond particles from methane-hydrogen gas", J. Material Sci. 17, 3106-3112(1982).

13. M. Sokolowski, A. Sokolowska, B. Gokieli, A. Michalski, A. Rusek and Z. Romanowski, "Reactive pulse plasma crystallization of diamond and diamond-like carbon", J. Crystal Growth, 47, 421-426(1979).
14. A. Sawabe and T. Inuzuka, "Growth of diamond thin films by electron-assisted chemical vapor deposition and their characterization", Thin Solid Films, 137, 89-99(1986).
15. Y. Hirose and Y. Terasawa, "Synthesis of diamond thin films by thermal CVD using organic compounds", Jap. J. Appl. Phys., 25(6), L519-L521(1986).
16. K. Suzuki, A. Sawabe, H. Yasuda and T. Inuzuka, "Growth of diamond thin films by dc plasma chemical vapor deposition", Appl. Phys. Lett. 50(12), 728-729(1987).
17. J. Tsacoyeanes and T. Feng, in "SPIE Proceedings: Diamond Optics," A. Feldman and S. Holly, ed.,,969, 138 (1988).
18. G. Saenz, K. Sun, and R. Shah, in "SPIE Proceedings: Diamond Optics," A. Feldman and S. Holly, ed.,, 969, 178 (1988).
19. A. Ono, T. Baba and A. Nishikawa, Jap. J. Appl. Phys. 25, L808 (1986).
20. Y. S. Touloukin, R. W. Powell, Y. C. Ho and S. C. Nickiou,"Thermo-physical properties of matter, Vol. 10: thermal diffusivity," p. 163, Plenum Publishing Corpn., New York (1973).
21. H. S. Carslaw and J. C. Jaeger,"Conduction of Heat in Solids," 2nd ed., p. 263 Clarendon, Oxford (1959).
22. R. M. Wood, Laser Damage in Optical Materials, Adam Hilger, Bristol (1986).
23. R. M. Walser, M. F. Becker and D. Y. Sheng, "Laser damage of crystalline silicon by multiple 1.06 μm picosecond pulses", in Laser Induced Damage in Optical Materials:1981, H. E. Bennet, et. al. ed., National Bureau of Standards Special Publication 638, 103-113 (1983)
24. D. H. Gill, B. E. Newman and J. McLeod, in National Bureau of Standard Special publication 509, 248(1977).

7. LIST OF PUBLICATIONS

1. S. Albin, A. D. Cropper, L. C. Watkins, C. E. Byvik and A. M. Buoncristiani, "Laser Damage Threshold of Diamond Films", Opt. Eng. Vol.28, March 1989, 281-285.
2. S. Albin, W. P. Winfree, and B. S. Crews,"Thermal diffusivity of Diamond Films Using a Laser Pulse Technique", J. Electrochem. Soc. Vol.137, June 1990, 1973-76.
3. S. Albin, A. D. Cropper, L. C. Watkins, C. E. Byvik , A. M. Buoncristiani, K. V. Ravi and S. Yokota, "Laser Damage of Diamond Film Windows", Diamond Optics, Proc. SPIE, Vol. 969, August, 1988, 186-193.
4. A. M. Buoncristiani, G. Armagan, C. E. Byvik and S. Albin,"Optical Materials for Space Based Laser Systems", Proc. SPIE Vol. 1118, March 1989, 25-34.